ZnCr2-xFexO4 Nanoparticles-Modified Electrochemical Sensors: A Comparative Study

$ZnCr_{2-x}Fe_xO_4$ Nanoparticles-modified electrochemical sensors: A comparative study

Mallikarjun Madagalam[1, 2,3] *, Mattia Bartoli[3,4], Sandro Carrara[2], Alberto Tagliaferro[1,3]

[1]Department of Applied Science and Technology, Politecnico di Torino, 10129 - Torino, Italy.
[2]Bio/CMOS Interfaces Laboratory, École Polytechnique Fédérale de Lausanne, 2000 - Neuchâtel, Switzerland.
[3]National Interuniversity Consortium of Materials Science and Technology (INSTM), 50121 - Florence, Italy.
[4]Center for Sustainable Future Technologies, Istituto Italiano di Tecnologia, 10144 - Torino, Italy.
*Corresponding author: mallikarjun.madagalam@polito.it

***Abstract*— This work presents the $ZnCr_{2-x}Fe_xO_4$ (x = 1, 1.25, 1.5, 1.75, 2) nanomaterials modified screen-printed carbon-based electrochemical sensors. The electrochemical sensor's performance was studied towards paracetamol sensing. The sensitivity and kinetic rate constant were evaluated for each sensor and compared. Found that the sensitivity and kinetic rate constant decreased as the amount of Cr decreased from x = 1 to 1.75. The best sensitivity and kinetic rate constant were observed for the pure ferrite sensor (x = 2).**

Keywords*— Nanoparticles, spinel, sensors, sensitivity, rate constant, paracetamol

I. Introduction

Paracetamol is the most widely used antipyretic drug to treat fever, headache, cold, migraine, and chronic pain in the world [1-3]. Paracetamol is also known as acetaminophen, N-acetyl-p-aminophenol, this is a very safe and effective agent when used within the limits; limited usage can avoid toxic metabolite accumulation and liver or kidney damage [4]. To avoid problems concerning paracetamol overdose or to understand the usage within the limits it is very important to have a reliable, low-cost, user-friendly sensing system. Among all the approaches, electrochemical sensing is a very simple, low-cost technique, easily employable in on-site applications [2, 5]. Developing new electrode materials to improve the sensing performance of electrochemical sensors is a wide research topic. For this purpose, several research studies used different nanomaterials to tailor the screen-printed carbon electrodes (SPCE) [6-8].

In this work, we focused on spinel-based ferrite nanomaterials as an electrochemical sensing platform. A spinel crystal structure is a face-centered cubic system with O anions forming tetrahedral and octahedral voids. Metallic cations have the tendency to occupy these voids depending on their oxidation states. Based on the occupancy of cations the spinel can be normal or inverse spinel [9-10]. In normal spinel ferrites, M(II) occupies the tetrahedral void and M(III) occupies the octahedral void [9]. Inverse spinel has octahedral voids occupied by M(II) and M(III) whereas tetrahedral voids are occupied by only M(III) [10]. There is not much research has been carried out on the application of spinel nanomaterials as electrochemical sensing species. In our previous work, we studied how the chemical composition and transition from normal spinel ($ZnFe_2O_4$) to inverse spinel ($NiFe_2O_4$) affect the electrochemical sensing performance [11]. How the electrochemical sensing be affected by replacing Fe(III) with Cr(III) and Bi(III) in the octahedral void of the $ZnFe_2O_4$ structure? was also partly studied [12].

The present paper presents the application of the Zn(II) based normal spinel nanomaterials as electrochemical sensing materials. We present the electrochemical sensing capability of $ZnCr_{2-x}Fe_xO_4$ (x = 1, 1.25, 1.5, 1.75, 2) nanomaterials by comparing the sensitivity and kinetic rate constant. Commercially available SPCEs were modified by synthesized spinel nanomaterials. The electrochemical sensing ability of the surface modified SPCEs was studied towards paracetamol. The sensitivity, and kinetic rate constant of different sensors are reported and discussed.

II. Materials and Methods

A. Chemicals

$Zn(NO_3)_2{\cdot}6H_2O$, $Cr(NO_3)_3{\cdot}9H_2O$, $Fe(NO_3)_3{\cdot}9H_2O$, $C(NH_2)_2O$ (Urea), $C_4H_{10}O$ (Butanol), and paracetamol powder were purchased from Sigma Aldrich and used without further modification.

B. Material synthesis

The auto-combustion method as described in the literature [13] was used to synthesize nanomaterials. $Zn(NO_3)_2{\cdot}6H_2O$, $Fe(NO_3)_3{\cdot}9H_2O$, $Cr(NO_3)_3{\cdot}9H_2O$, were acted as oxidizing agents, and $C(NH_2)_2O$ (Urea) as a reducing agent. A redox mixture of 1:1 mole ratio was prepared in a crucible, inserted inside a graphite reactor, and heated up to 600 °C within a furnace. The resulting product was annealed at 600 °C for 1hr and cooled down at normal conditions until the material reached room temperature. The final material was grounded to obtain fine powders of $ZnCr_{2-x}Fe_xO_4$ (x = 1, 1.25, 1.5, 1.75, 2).

C. Electrodes modification

Commercially available screen-printed carbon working electrode (0.12 cm^2) (WE), carbon counter electrode (CE), and Ag/AgCl reference electrode (RE) were used as three electrodes in the electrochemical system. Nanomaterial suspension was prepared (3:1 material to solvent ratio) in

butanol. 5 µL of nanomaterial suspension was spread over the WE surface and dried overnight (drop casting technique) at room temperature.

D. Electrochemical measurements

Bio-logic SP-300 potentiostat was used to perform cyclic voltammetry (CV) measurements. 100 µL solution of 1mM paracetamol (0.1M PBS at pH 6.9) was dropped on top of the electrochemical system by setting the potentiostat to sweep the voltage range from –0.6 to +0.8 V (versus Ag/AgCl). Faradaic redox currents and potentials were evaluated after subtracting the non-Faradaic current from the peak current and positions of cyclic voltammograms. Cyclic voltammograms were recorded by varying the scan rate from 50 – 300 mV/s (steps of 50 mV/s) to understand the electron transfer process at the electrochemical interface. In order to construct the calibration, CV was also done using paracetamol concentrations ranging from 0.5 mM to 3 mM in steps of 0.5 mM at a scan rate of 100 mV/s. The sensitivity of the sensor was then determined by taking the calibration's slope. MATLAB was used for all data processing and graphing.

III. RESULTS AND DISCUSSION

A. Materials Characterization

A Zeis SupraTM 50 field emission scanning electron microscope (FE-SEM) was used (Oberkochen, Germany). Fig.1 display the FE-SEM images of $ZnCrFeO_4$. It was proven that the produced particles are spherical and less than 100 nm in size (nanoparticles) and that some sort of particle aggregation can be seen. We observed the same for the other materials too because of the same synthesis process used. The particle sizes evaluated from the respective SEM images by ImageJ are reported in Table 1. We observe that the size of the nanoparticles varies between 20 to 50 nm.

Table 1. The particle size of nanomaterials.

Material	Particle size (nm)
$ZnCrFeO_4$	26 ± 7
$ZnCr_{0.75}Fe_{1.25}O_4$	26 ± 5
$ZnCr_{0.5}Fe_{1.5}O_4$	25 ± 5
$ZnCr_{0.25}Fe_{1.75}O_4$	29 ± 6
$ZnFe_2O_4$	44 ± 17

B. Electrochemical characterization

The recorded cyclic voltammograms of six different sensors for 1 mM paracetamol in 0.1 mM PBS at pH 6.9 (scan rate (ν) = 100 mV/s) are shown in Fig. 2. In comparison to the bare sensor, $ZnCr_{2-x}Fe_xO_4$ (x = 1, 1.25, 1.5, 1.75, 2) nanoparticle-based sensors produced better results. In contrast to other sensors, the $ZnFe_2O_4$ sensor produced the maximum oxidation current of 52.41 ± 0.56 µA at the lowest oxidation potential of 244 ± 1 mV. As shown in Table 2, the presence of Cr(III) in the sensing material has reduced significantly the oxidation current compared to the pure $ZnFe_2O_4$ sensors with slight differences in potential.

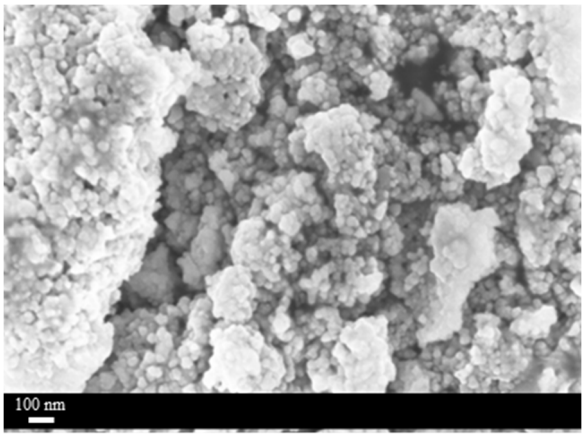

Fig. 1. FE-SEM image of $ZnCrFeO_4$.

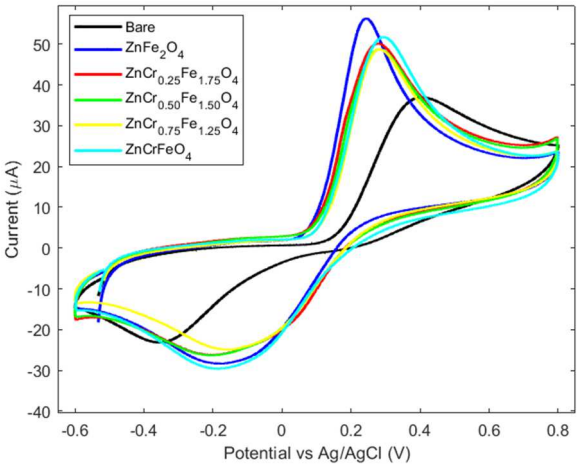

Fig. 2. Cyclic voltammograms of different sensors with 1 mM paracetamol in 0.1 M PBS at pH 6.9 (ν = 100 mV/s).

The $ZnCrFeO_4$ sensor's cyclic voltammograms at various 'ν' between 50 and 300 mV/s with 1 mM paracetamol in 0.1 M PBS (pH 6.9) are shown in Fig.3. As the scan rate is increased, it can be noticed that the oxidation and reduction currents are growing while the peak positions are shifting. According to the Randles-Sevčik equation [14], as shown in the inset of Fig. 3 together with the linear regression equations, the oxidation and reduction peak currents increase linearly with '$\sqrt{\nu}$'. Since all the sensors showed the same behavior, we can infer that the electrochemical sensors under investigation are freely diffusing quasi-reversible electrochemical systems.

The positions of the oxidation and reduction peaks (E_{pa} and E_{pc}) were plotted versus ln(ν) in Fig. 4 using the data from the cyclic voltammograms taken at various scan rates. The anodic and cathodic slopes were evaluated using linear fitting, and Fig. 4 reports the linear regression equations with the fitting coefficient R^2. Peak-to-peak separation ΔEp with respect to ln(ν) is shown in the inset of Fig. 4, and it exhibits a strong linear connection with R^2 = 0.9966. The electron transfer rate coefficient abbreviated as "α" was determined using the Laviron model [15]. According to the literature [2], the reaction requires 'n' electrons, where '2' was chosen as the number of electrons that participated. As the mechanism is not totally reversible, ΔEp changes with the scan rate. To enable meaningful comparisons between sensors, the ΔEp value was set at 100 mV/s. Table 1 lists the results of the Laviron equation's calculation of the first-order kinetic rate-

Table 2. Electrochemical parameters of $ZnCr_{2-x}Fe_xO_4$ and bare sensors.

Sensor	Ox. Potential (mV)	Ox. Current (μA)	α	ΔE_p (mV)	k (ms^{-1})	Sensitivity (μA/mM)
Bare	396 ± 2	34.50 ± 0.20	0.543 ± 0.003	746 ± 5	$2.29 \pm 0.27 \cdot 10^{-3}$	16.68 ± 0.93
$ZnCrFeO_4$	285 ± 2	47.68 ± 0.72	0.24 ± 0.01	446 ± 2	4.53 ± 0.54	35.72 ± 0.11
$ZnCr_{0.75}Fe_{1.25}O_4$	282 ± 2	45.88 ± 0.39	0.355 ± 0.003	564 ± 7	0.175 ± 0.028	34.48 ± 0.15
$ZnCr_{0.5}Fe_{1.5}O_4$	285 ± 2	45.92 ± 0.12	0.35 ± 0.01	455 ± 4	1.1 ± 0.06	32.93 ± 0.27
$ZnCr_{0.25}Fe_{1.75}O_4$	280 ± 1	47.81 ± 0.26	0.32 ± 0.01	488 ± 4	0.88 ± 0.16	32.07 ± 0.15
$ZnFe_2O_4$	244 ± 1	52.41 ± 0.56	0.23 ± 0.02	386 ± 2	13.1 ± 2.8	37.75 ± 0.17

constant 'k'. We can see from Table 1 that the $ZnFe_2O_4$ sensor has the lowest ΔEp, and greatest k, indicating a high likelihood of reversibility and quicker response at the interface. All other sensors exhibit greater 'k' values when compared to the bare sensor, demonstrating the interface's decreased reaction time.

By changing the paracetamol concentration, the CV was carried out three times for each sensor. To build the calibration for each type of sensor, linear fitting was done using the average oxidation current at each concentration, as shown in Fig. 5. The sensitivity of each sensor to detect paracetamol was determined by the slope of the linear calibration fit, and this information is presented in Table 1. It is observed that the sensitivity has reduced as the amount of Cr decreased from x = 1 to 1.75 and increased for the $ZnFe_2O_4$ sensor. This demonstrates that the presence of Cr in $ZnFe_2O_4$ is arguably affecting the electrochemical performance.

C. Conclusion

As a result, we were able to effectively develop a variety of zinc-based nanomaterials by inserting Cr into the structure. The sensing performance of the six different normal spinel nanomaterials was demonstrated electrochemically. The change in the amount of Cr in $ZnFe_2O_4$ is appreciably affecting the sensitivity and kinetic rate constant in comparison to the bare carbon sensor.

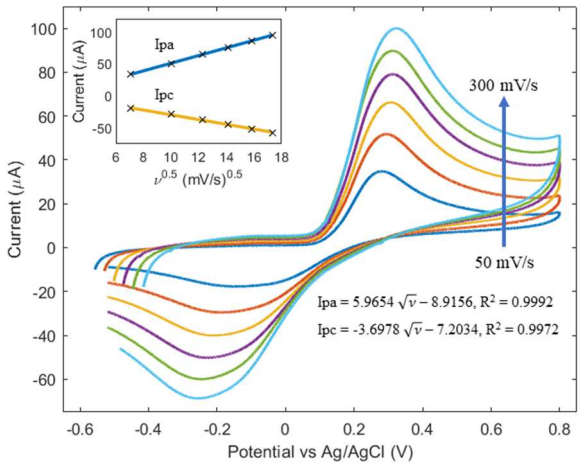

Fig. 3. Cyclic voltammograms of $ZnCrFeO_4$ sensor at different 'ν' with 1mM paracetamol in 0.1M PBS pH 6.9. The inset shows the redox currents with respect to $\nu^{0.5}$.

To understand the effect clearly, further nanomaterial characterization is needed. Nanomaterials bandgap, specific surface area, and electroactive surface area can remarkably affect the electrochemical sensing performance. Ionic radii and the spin of Cr and Fe with O may play a role too in describing their performance in sensing. The outcome of sensors has good electrochemical sensing capability; as a result, it is suggested that they can be utilized in biosensors to monitor additional molecules of biomedical relevance.

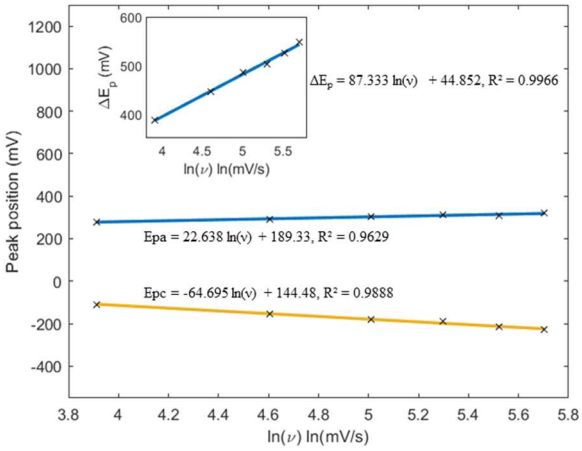

Fig. 4. Linear fitting of E_{pa} and E_{pc} of $ZnCrFeO_4$ sensor with ln(ν), inset: ΔEp vs ln(ν).

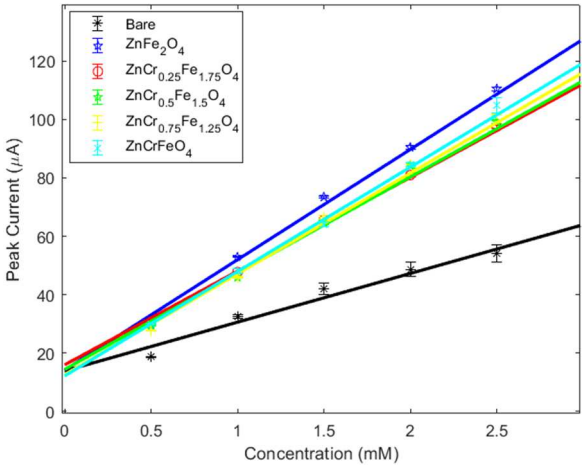

Fig. 5. Calibration of $ZnCr_{2-x}Fe_xO_4$ (x = 1, 1.25, 1.5, 1.75, 2) sensors compared with the bare sensor.

IV. REFERENCES

[1] R. M. de Carvalho, R. S. Freire, S. Rath, and L. T. Kubota, "Effects of EDTA on signal stability during electrochemical detection of acetaminophen," *J. Pharmaceutical Biomed. Anal.*, vol. 34, no. 5, pp. 871–878, 2004.

[2] Kang, X.; Wang, J.; Wu, H.; Liu, J.; Aksay, I.A.; Lin, Y. "A graphene-based electrochemical sensor for sensitive detection of paracetamol," *Talanta* 2010, 81, 754–759.

[3] Li, J.; Liu, J.; Tan, G.; Jiang, J.; Peng, S.; Deng, M.; Qian, D.; Feng, Y.; Liu, Y. "High-sensitivity paracetamol sensor based on Pd/graphene oxide nanocomposite as an enhanced electrochemical sensing platform," *Biosens. Bioelectron*. 2014, 54, 468–475.

[4] M. Li and L. H. Jing, "Electrochemical behavior of acetaminophen and its detection on the PANI–MWCNTs composite modified electrode," *Electrochim. Acta*, vol. 52, no. 9, pp. 3250–3257, 2007.

[5] Li, M.; Wang,W.; Chen, Z.; Song, Z.; Luo, X. "Electrochemical determination of paracetamol based on Au@ graphene core-shell nanoparticles doped conducting polymer PEDOT nanocomposite," *Sens. Actuators B Chem.* 2018, 260, 778–785.

[6] Madagalam, M.; Bartoli, M.; Tagliaferro, A.; Carrara, S. "Bismuth-nanocomposites modified SPCEs for non-enzymatic electrochemical sensors," *IEEE Sens. J*. 2021, 21, 11155–11162.

[7] J. Wang, J. Lu, S. B. Hocevar, and B. Ogorevc, "Bismuth-coated screen printed electrodes for stripping voltammetric measurements of trace lead," *Electroanalysis*, vol. 13, no. 1, pp. 13–16, Jan. 2001.

[8] N. Aliakbarinodehi *et al.*, "Electrochemical nanostructured biosensors: Carbon nanotubes versus conductive and semi-conductive nanoparticles,"*Chem. Papers*, vol. 69, no. 1, pp. 134–142, Jan. 2015,

[9] Gabriela R. Ferracutti, M. Florencia Gargiulo, M. Luján Ganuza, Ernesto A. Bjerg, and Silvia M. Castro. "Determination of the spinel group end-members based on electron microprobe analyses," *Miner Petrol* (2015) 109:153–160.

[10] P.R. Graves, C.Johnston and J.J.Campaniello. "RAMAN SCATTERING IN SPINEL STRUCTURE FERRITES," *Mat. Res. Bull.* 23:1651-1660, 1988.

[11] Madagalam.M, Bartoli.M, Rosito.M, Blangetti.N, Etzi.M, Padovano.E, Bonelli.B, Carrara.S, Tagliaferro.A. "Unraveling the effect of the chemical and structural composition of $Zn_xNi_{1-x}Fe_2O_4$ on the Electron Transfer at the Electrochemical Interface," *Small Struct*. 2023, 2300163.

[12] Madagalam.M, Bartoli.M, Carrara.S, Tagliaferro.A. "$ZnM_xFe_{2-x}O_4$ (M=Cr, Bi) Nanoparticles-modified electrochemical sensors: Effect on sensitivity and first-order kinetic rate constant," *IEEE Biosensors Conference*, London, July-August 2023.

[13] A. C. F. M. Costa, E. Tortella, M. R. Morelli, M. Kaufman, and R. H. G. A. Kiminami. "Effect of heating conditions during combustion synthesis on the characteristics of $Ni_{0.5}Zn_{0.5}Fe_2O_4$ Nanopowders," *JOURNAL OF MATERIALS SCIENCE* 37 (2002) 3569 – 3572.

[14] A. J. Bard and L. R. Faulkner, *Electrochemical Methods Fundamentals and Applications*. New York, NY, USA: Wiley, 2001.

[15] Laviron, "General expression of the linear potential sweep voltammogram in the case of diffusion less electrochemical systems," *J. Electroanal.Chem. Interfacial Electrochem.*, vol. 101, no. 1, pp. 19–28, Jul. 1979.